Shallow magma diversions during explosive diatreme-forming eruptions

Nicolas Le Corvec[1], James D. Muirhead[2] and James D. L. White[3]

[1] **Laboratoire Magmas et Volcans, Université Clermont Auvergne - CNRS - IRD, OPGC, Clermont-Ferrand, France**
[2] **Department of Earth Sciences, Syracuse University, Syracuse, New York, USA**
[3] **Geology Department, University of Otago, Dunedin, New Zealand**

nicolas.le_corvec@uca.fr

Introduction

Recent field and geophysical studies have revealed **complex networks** of sub-vertical **dikes** to sub-horizontal **sills** underlying monogenetic volcanic fields *[Kiyosugi et al., 2012; van Wyk de Vries et al., 2014; Richardson et al., 2015; Muirhead et al., 2016; McLean et al., 2017]*, with the growth of these networks affecting the location and style of eruptive activity.

Hazardous vent-site shifts are documented for explosive **phreatomagmatic eruptions** resulting from lateral magma diversion during growth of dike and sill feeders *[Lefebvre et al., 2012; Muirhead et al., 2016]*.

Magma diversions and transitions in intrusion geometries can be explained by several physical and structural factors, such as mechanical contrasts *[Kavanagh et al., 2006]*, pre-existing fractures *[Le Corvec et al., 2013]*, and stress loading/unloading *[Maccaferri et al., 2014]*.

Field observations of lateral magma diversion in maar-diatreme fields

Recent studies field and seismic reflection studies have documented lateral magma diversions, particularly in sills, related to monogenetic volcanoes (**Fig. 1**) *[Németh and Martin, 2007; Valentine and van Wyk de Vries, 2014; Re et al., 2015; Richardson et al., 2015; Muirhead et al., 2016; Fierstein and Hildreth, 2017; McLean et al., 2017; van den Hove et al., 2017]*.

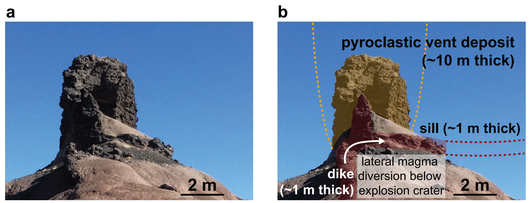

Figure 1: Example of a dike transitioning to a sill intrusion immediately below an eruptive conduit in the Hopi Buttes volcanic field (Arizona). In the photo (lat. 35.10406°N, long. 110.30943°W) provided (a and b), no cross-cutting relations are observed between the dike, sill, and conduit. The scale provide is in reference only to the foreground of the photo. Dashed lines in b represent an interpreted projection of the vent and sill prior to erosion.

No studies to date have modelled how topographic and material changes resulting from explosive, crater-forming eruptions influence the development of underlying feeder systems.

Here we utilize, for the first time, **finite element modeling** to analyze the evolution of stress states during explosive **excavation** and **filling** of gravitationally loaded country rock during maar-diatreme volcanism. This methodology allows us to test **how local stress fields, and therefore magma propagation, respond to the mechanical changes produced by excavation and filling of maar-diatreme structures**.

Methodology

We use finite element models through **COMSOL Multiphysics®** to investigate the effects of diatreme **excavation** for single-explosion craters and **infilling** on the local state of stress (**Fig. 2**). These stress changes are expected to affect the geometry of surrounding intrusions, which form normal to the least compressive stress *[Anderson, 1951]*. The **2D axisymmetric elastic domain** has a Young's Modulus (E_C) of 15 GPa (sandstone equivalent), a density (ρ_C) of 2300 kg.m^{-3}, and Poisson's ratio (μ) of 0.25. The area of the elastic domain is 100 × 100 km to avoid side effects, and is subjected to gravitational loads expressed by 1) an **initial lithostatic stress** *[Grosfils, 2007]*.

$$\sigma_r = \sigma_\theta = \sigma_z = -\rho_C \cdot Z \cdot g$$

where Z is negative downward and negative stress values indicate compression, and g is the Earth's gravitational acceleration (-9.81 m.s^{-2}), and 2) a **body load**

$$\rho_C \cdot g$$

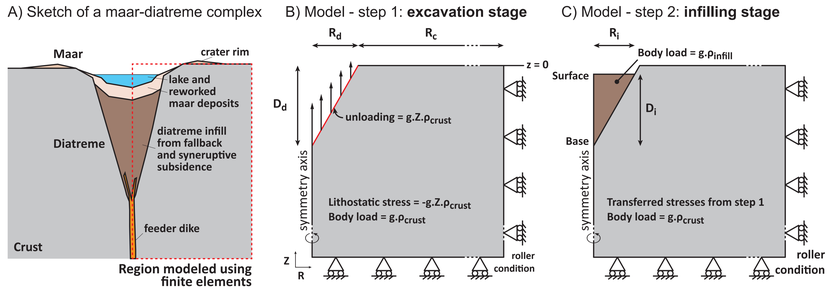

Figure 2: Finite element model (FEM) configuration. A) Sketch of a maar-diatreme complex. Modified from *[Lorenz, 1986]*. The dotted red square represents the area modeled numerically using an axisymmetric axis. B) The initial step models the excavation stage. The model is gravitationally loaded with a lithostatic pre-stress and a body load. A vertical load acting on the diatreme's wall represents the mass of rock excavated. C) The second step models the infilling stage. The initial stress conditions and geometry are transferred from the initial step. The diatreme is filled with either 25, 50 or 75% of the total diatreme volume by volcanoclastic material (E_i = 10 GPa, ρ_i = 2000 kg.m^{-3}, and μ = 0.25).

The diatremes were initially modeled as inverted cones: the depth to base of the diatreme and angle of the diatreme walls varied from 500-2000 m and 60-80°, respectively.

In the first step, an **unloading force** representing the missing vertical rock load is applied at the surface of the diatreme (red line in **Fig. 2B**) *[Maccaferri et al., 2014]*.

The second step of each model tested the effects of **infilling** of the diatreme after excavation (**Fig. 2C**). Their initial conditions (deformed geometry and state of stress) corresponds to the **transferred solution of the initial model** using COMSOL capabilities.

Results

The differential tectonic stress state ($\Delta\sigma_{tect} = \sigma_r - \sigma_z$) affects the driving forces for vertical magma movements *[Rubin, 1995]*. **Negative values** = horizontal compression ($\sigma_z > \sigma_r$) (e.g., in red Fig. 3b), which **discourages vertical magma propagation** in dikes and promotes lateral propagation in sills *[Menand et al., 2010]*. **Positive values** = horizontal extension ($\sigma_r > \sigma_z$), which **favor vertical magma propagation** (e.g., in blue Fig. 3b).

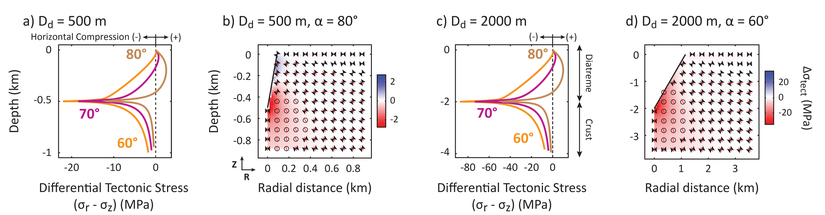

Figure 3: State of stress within the crust surrounding the newly-formed diatreme. a and c) Differential tectonic stress along the diatreme flank and in the underlying crust for different wall dips (α = 80, 70 and 60°) and for different diatreme depths (D_d). b and d) Differential tectonic stress and stress orientation within the crust. Blue and red shadings represent extensional and compressional $\Delta\sigma_{tect}$, respectively. The hourglass shapes are oriented along the direction of greatest compressive stress (σ_1); the red bars along the direction of least compressive stress (σ_3). Circles represent an out-of-the plane hourshape glass (σ_1 perpendicular to the r – z plane).

Results - Stress states during maar-diatreme formation

Excavated diatreme structures with steep diatreme walls exhibit horizontal extension in the upper part of the diatreme walls (positive values and blue shading in **Fig. 3b**), while the lower part, as well as the underlying host rock, are subjected to horizontal compression (negative values and red shading in **Fig. 3**).

Wider diatremes (e.g., 60° dip) show a decrease in the area subjected to horizontal extension and an increase in the area of horizontal compression in the lower part of the diatreme and underlying crust (**Fig. 3**).

The orientation of σ_3 is vertical below the excavated diatreme and in the modeled r-z plane rotates in an anticlockwise manner to sub-horizontal in the surrounding crust (red lines **Figs. 3b and d**). Directly below the surface, σ_3 rotates again and becomes oriented out of the plane (hourglasses without red lines **Figs. 3b and d**).

Diatreme infills exhibit horizontal extension at their base, and horizontal compression near the pre-eruption ground surface (**Figs. 4a-b**).

Differential tectonic stress magnitudes are dependent on the volume of the infill.

Horizontal compression occurs in country rock below the diatreme, but with differential tectonic stress magnitude reaching only ~-2 MPa. Horizontal extension occurs near the contact between the diatreme wall and the infill, with differential tectonic stress values up to ~65 MPa (**Fig. 4b**).

The orientation of σ_3 within the infill is horizontal in its lower half, and vertical in the upper half. Within the surrounding host rock, the orientation of σ_3 is vertical below the diatreme and rotates to sub-horizontal in the vicinity of diatreme walls up to the surface (**Figs. 4c-f**).

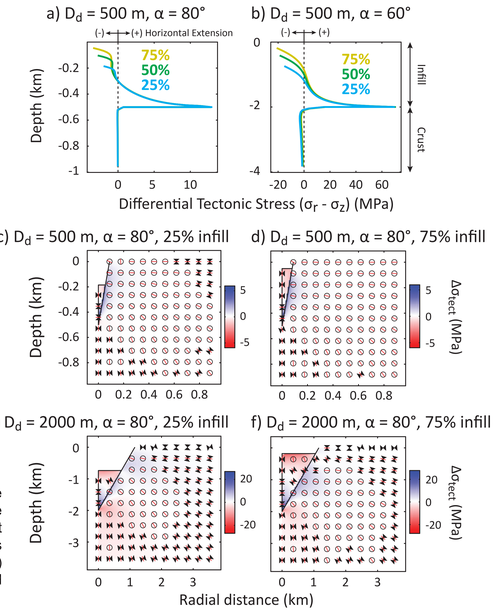

Figure 4: State of stress within the diatreme's infill and within the surrounding crust. a and b) Differential tectonic stress along the symmetrical axis of the model (left boundaries) for different diatreme's depth (D_d), dipping angles (α), and infill volume (colors blue, green and yellow for 25, 50, 75% of infill, respectively). c to f) Differential tectonic stress and stress orientation within the infill and the crust. Legend as in **Fig. 3**.

Conclusions

Phases of explosive excavation encourage magma to stall in sills below the excavated structure, allowing for lateral changes in the position of fragmentation zones early in the diatreme's history rather than progressive deepening (**Fig. 5a**).

Subsequent infilling promote magma ascent to shallower levels within the diatreme. Horizontal compression in the upper diatreme drives lateral magma diversions, encouraging explosive diatreme widening and growth at shallow depths (**Fig. 5b**).

Compressional stresses resulting from increasing infill volumes during continued diatreme growth are expected to promote sill-driven lateral quarrying, nest-diatreme formation, and larger explosive activity in well-developed examples (**Fig. 5b**).

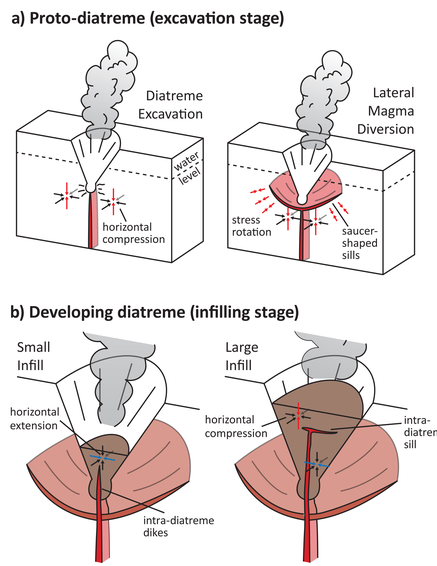

Figure 5: Sketch of a maar-diatreme eruption and formation of the magmatic plumbing system during a) the proto-diatreme (aka **excavation** stage) and b) developing diatreme (aka **infilling** stage). The colored arrows represent the orientation of the minimum compressional stress (σ_3), the blue and red colors represent the differential tectonic stress, extensional and compressional, respectively.